J Mater Sci (2011) 46:2622–2626
DOI 10.1007/s10853-010-5116-x

TiO_2/graphene composite from thermal reaction of graphene oxide and its photocatalytic activity in visible light

Yupeng Zhang · Chunxu Pan

Received: 29 September 2010 / Accepted: 24 November 2010 / Published online: 7 December 2010

Abstract In this study, the P25 TiO_2 nanoparticles and graphene sheets (GSs) composite were prepared from a facile thermal reaction of graphene oxide. Its microstructures and photocatalytic properties were characterized and measured using X-ray diffraction (XRD), high resolution transmission electron microscopy (HRTEM), Brunauer–Emmett–Teller (BET) specific area analysis, X-ray photoelectron spectroscopy (XPS), FT-IR spectra, and ultraviolet–visible (UV–vis) diffuse reflectance spectroscopy. Compared with pure P25 nanoparticles, the results reveal that (1) there is a red shift about 20 nm in the absorption edge of the P25/graphene composite; (2) the photocurrent of the composite is about 15 times higher than that of pure P25; (3) the visible light photocatalytic activity of the composite is enhanced greatly on decomposition of methylene blue (MB). The photocatalytic mechanism of the P25/graphene composite is also discussed.

Introduction

As the most promising photocatalyst, TiO_2 has been expected to play an important role in environmental pollution control, solar energy and so on. Up to now, various processes have been proposed via either doping or modification to narrow its band gap and enhance the photocatalytic activity under the visible light radiation [1–4].

In recent years, as a two-dimensional (2D) crystal which is made up of sp^2-hybridized carbon atoms, graphene has been widely investigated due to its unique physical and chemical properties, such as high thermal conductivity (5000 Wm^{-1} K^{-1}) [5], high charge carrier mobility (15000 cm^2 V^{-1} s^{-1}) at room temperature [6], high specific surface area up to 2630 m^2 g^{-1} [7], and complex band structure with conduction and valence bands overlapping for a multi-layer graphene more than three layers [8]. Therefore, the composite of graphene and semiconductors especially TiO_2 nanoparticles [9–12] are currently being considered as potential photocatalyst in air and water purification. Zhang et al. [11] prepared a chemically bonded TiO_2 (P25)–graphene nanocomposite using hydrothermal reaction. They found that the composites exhibited a significant enhancement in reaction rate when comparing to the bare P25 and P25-CNTs with the same carbon content during photodegradation of methylene blue (MB). Zhang et al. [12] synthesized variant TiO_2/graphene composites with different graphene content by sol–gel method and indicated that the highest photocatalytic activity was the sample with 5% graphene sheets (GSs). Obviously, graphene is a promising candidate for developing high performance photocatalysts.

In this paper, we will introduce a process for preparing the TiO_2(P25)/graphene composite from reduction of graphene oxide (GO) by heat treatment. We expect this process also dope the carbon (C) atoms into TiO_2 which will remarkably improve the visible light photocatalytic activity.

Y. Zhang · C. Pan
School of Physics and Technology and Key Laboratory of Artificial Micro- and Nano-Structures of Ministry of Education, Wuhan University, Wuhan 430072, People's Republic of China

C. Pan (✉)
Center for Electron Microscopy, Wuhan University, Wuhan 430072, People's Republic of China
e-mail: cxpan@whu.edu.cn

Experimental

Synthesis of graphene oxide

The graphene oxide was synthesized from natural graphite powder (99.95%,32 μm) by the modified Hummers method [13, 14]. That is (1) The graphite powder (0.3 g) was put into the solution containing 2–4 mL concentrated H_2SO_4, 0.5 g $K_2S_2O_4$, and 0.5 g P_2O_5. The resultant dark blue mixture was kept stirring for 4 h at 80 °C, and then was carefully diluted with distilled water, the initial product was obtained by filtering and drying at ambient temperature. (2) The initial product was re-dispersed into 12 mL concentrated H_2SO_4, and 1.5 g $KMnO_4$ was added laggardly. During the processing, an ice bath should be used to avoid the temperature increasing over 20 °C. (3) The mixture was stirred at 35 °C for 2 h, and 25 mL distilled water was added. (4) 70 mL distilled water and 2 mL 30% H_2O_2 solution were added, and the reaction was terminated in 15 min. Then the color of the mixture was changed from snuff color to bright yellow. (5) At last, the mixture was washed by HCl solution and distilled water in turn until the pH value of rinse water became neutral, and the GO was obtained after drying.

Synthesis of the P25/graphene composite

The TiO_2 (P25) nanoparticles (80% anatase + 20% rutile) were purchased from Degussa. 10 mg of GO and 90 mg of P25 were added into 100 mL distilled water. After 1 h sonication, the mixture was centrifuged and then dried at 30 °C. Finally, the obtained product was calcined at 300 °C for 2 h under argon atmosphere with the heating rate 100 °C min^{-1} [15, 16]. The P25/graphene composite was prepared during the process of reduction of the GO.

Characterizations

The crystal phases of the P25 and P25/graphene composite were measured using X-ray diffractometer (XRD) (D8 Advanced XRD, Bruker AXS, Germany) with Cu Kα radiation. The microstructures were observed by a HRTEM (JEM 2010FEF HRTEM, JEOL, Japan). The BET specific surface area was taken with a JW-BK surface area and pore size distribution analyzer (JWGB Sci. & Tech. Co, Ltd, Beijing). X-ray photoelectron spectroscopy (XPS) measurements were performed in a VG Multilab2000 spectrometer to obtain the information on chemical binding energy of the photocatalysts. The functional group of the GO, P25, and P25/graphene composite was detected using a Fourier transform infrared (FTIR) spectrometer (Nicolet is10, Thermo Fisher, America). The UV–vis diffuse reflectance spectra of the P25 and P25/graphene were obtained using an UV–vis spectrophotometer (UV-2550, Shimadzu, Japan).

Photocurrent experiments

In brief, 5 mg of the P25 and P25/graphene composite were dispersed in 5 mL ethanol, respectively. After 30 min sonication, the slurries were dip-coated onto a 1 × 2 cm indium–tin oxide (ITO) glass electrode and dried at 30 °C. The prepared photocatalyst/ITO electrodes, saturation calomel electrode, and platinum electrode were chosen as the working electrode, reference electrode, and counter electrode, respectively. The electrolyte was the 0.5 mol L^{-1} Na_2SO_4 aqueous solution. The working electrode was irradiated horizontally by a high pressure mercury lamp (160 W) and a cutoff filter ($\lambda > 400$ nm). The distance between working electrode and light source was 15 cm. The photocurrent tests of photocatalysts were measured using the electrochemical workstation (CHI660C, Chenhua, China).

Photocatalytic experiments

A 250 W high pressure mercury lamp and a cutoff filter ($\lambda > 400$ nm) were used as the light source for photocatalytic reaction. The photocatalytic activity of the photocatalysts was evaluated by decomposition of MB. 100 mg of photocatalysts was dispersed into 100 mL water solution containing 12 mg L^{-1} MB, and then the mixture was stirred incessantly under the light with a distance of 25 cm. The concentration of methyl blue was measured by a UV–vis spectrophotometer for every 60 min.

Results and discussion

Figure 1a illustrates the X-ray diffraction (XRD) patterns of P25 and the P25/graphene composite. Clearly, both materials exhibit the similar XRD patterns, and no graphene diffraction peaks were observed due to extremely small amount of graphene in the composite [11]. Figure 1b shows the TEM image of the P25/graphene composite, the GSs and TiO_2 nanoparticles can be clearly observed. HRTEM observation reveals that the TiO_2 nanoparticles are mostly covered with GS which consists of less than a few layers, as shown in Fig. 1c.

FT-IR spectra, as shown in Fig. 1d, reveal that GO presents the peaks of C–O (ν_{c-o}, 1045 cm^{-1}), C–O–C (ν_{c-o-c}, 1250 cm^{-1}), C–OH (ν_{C-OH}, 1365 cm^{-1}), C=O ($\nu_{C=O}$, 1720 cm^{-1}) in carboxylic acid [17, 18], and a broad peak at the range of 3000–3500 cm^{-1} which is attributed to the O–H stretching vibrations of the C–OH groups and water [14]. However, in the spectrum of the P25/graphene composite, these peaks totally disappeared, which

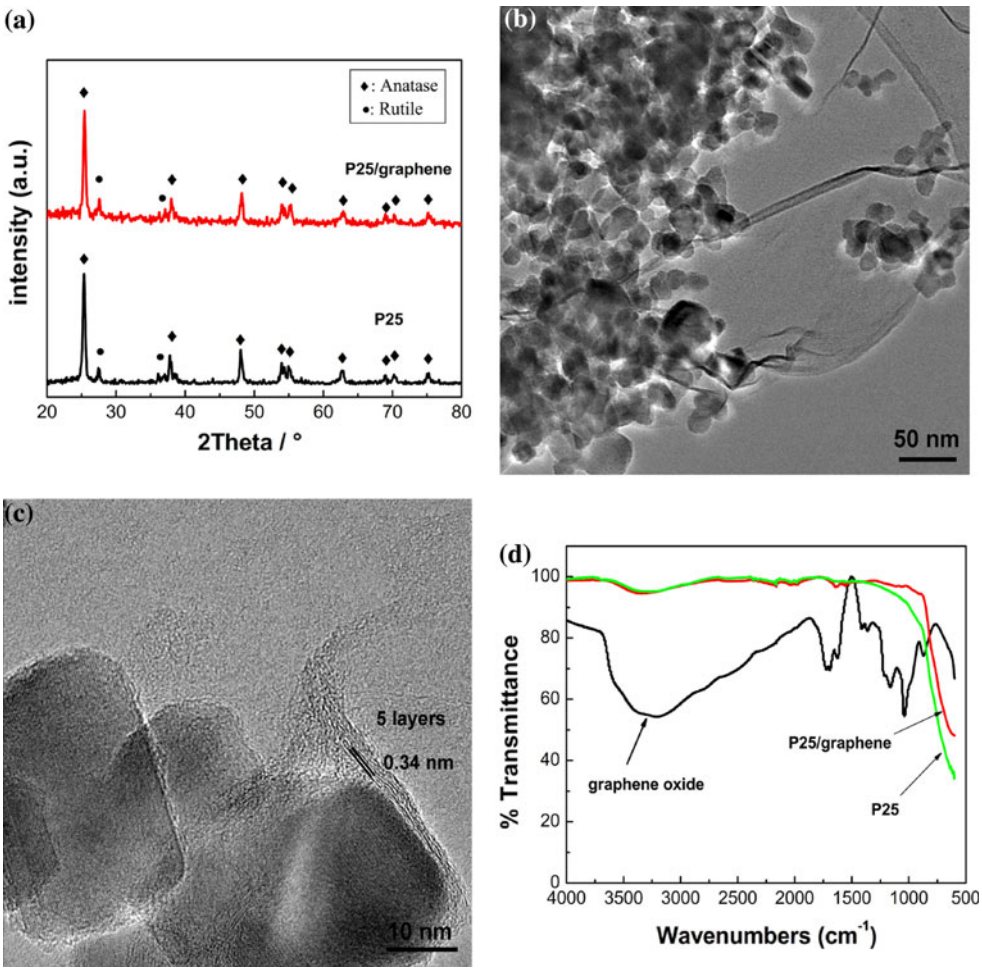

Fig. 1 **a** XRD patterns of the P25 and P25 TiO_2/graphene composite. **b** and **c** HRTEM images of the P25 TiO_2/graphene composite. **d** Fourier transform infrared (FTIR) spectra of the graphene oxide, P25, and P25 TiO_2/graphene composite

demonstrates that all oxygen-containing functional groups were completely removed through the thermal reaction. This indicates a possibility of compounding between P25 and graphene. Meanwhile, for the P25/graphene composite, the broad absorption at low wavenumbers (below 1000 cm^{-1}) is attributed to the vibration of Ti–O–Ti bonds in TiO_2, and the absorption peak around 1600 cm^{-1} is contributed by the skeletal vibration of the GSs.

According to the XPS survey spectrum, as shown in Fig. 2a, the P25/graphene composite contains only Ti, O, and C with the chemical binding energies of Ti 2*p*3/2 (458.6 eV), O 1*s* (523.0 eV), and C 1*s* (284.7 eV), respectively. In order to investigate the carbon states in the sample, we measured the C 1*s* core levels. Deconvolution of the C 1*s* peak in the XPS spectrum (Fig. 2b) shows the presence of two types of carbon bonds, that is, C–C (284.7 eV) and Ti-O–C (288.1 eV) [19–21]. The presence of the Ti–O–C structure revealed that the C atoms have substituted some of the Ti atoms in the TiO_2 lattice during the composite preparation.

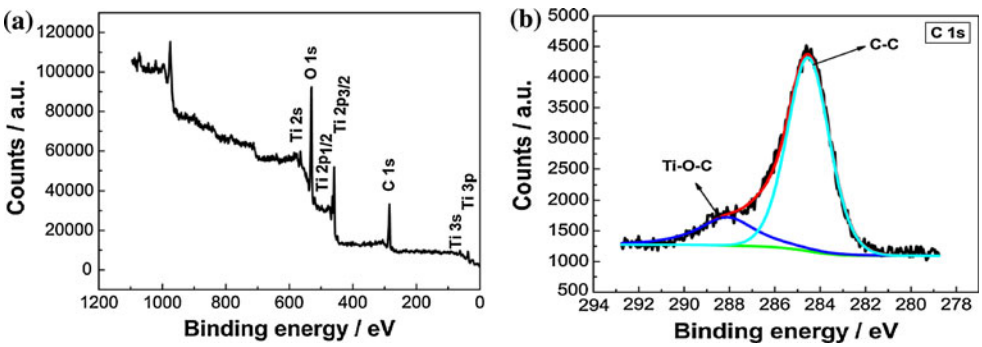

Fig. 2 XPS spectra of the P25 TiO_2/graphene composite. **a** survey spectrum and **b** C 1*s* spectrum

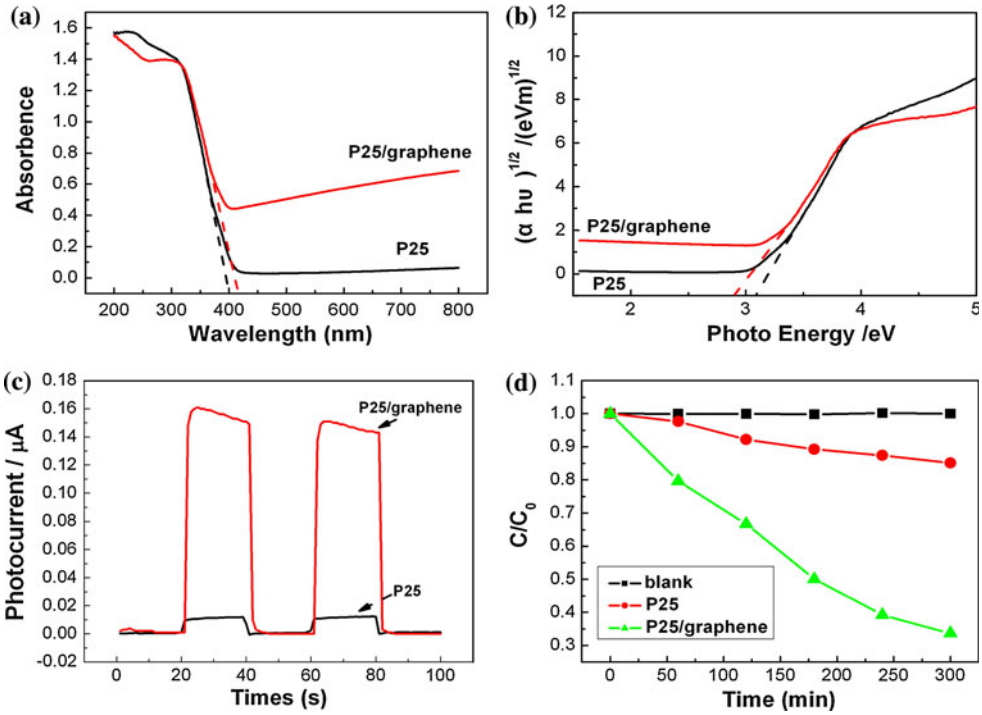

Fig. 3 **a** UV–vis absorption spectra and **b** curve of $(\alpha h\upsilon)^{1/2}$ versus photon energy of the P25 TiO_2 and P25 TiO_2/graphene composite. **c** Photoelectrochemical responses of the P25 TiO_2 and P25 TiO_2/graphene composite with a cutoff filter ($\lambda > 400$ nm). **d** Methylene blue decomposition upon visible light irradiation of the P25 TiO_2 and P25 TiO_2/graphene composite

Figure 3a gives the UV–vis absorption spectra of the pure P25 and P25/graphene composite. Obviously, the P25/graphene composite exhibits not only a red shift of 20 nm in the absorption edge but also a strong absorption in the visible light range. According to the Kubelka–Munk equation [22]:

$$\alpha h\upsilon = \text{const}(h\upsilon - E_g)^2$$

where $\alpha = (1 - R)^2/2R$, $R = 10^{-A}$ and A is an optical absorption. The band gap of photocatalyst can be calculated from the equation. Figure 3b plots the relationship of $(\alpha h\upsilon)^{1/2}$ versus photon energy, which shows that the band gap of pure P25 is 3.10 eV, whereas the band gap of the P25/graphene composite has been slightly reduced to 2.95 eV. This phenomenon can be explained as follows: during heat treatment of the GO, the functional groups on the surface of the GO (i.e. –OH, –COOH, and so on) disappeared. Upon this situation, the π electron of the carbon atom did not entirely bond with others to form the delocalized large π bond, and some unpaired π electrons bonded with the free electrons on the surface TiO_2 to form a Ti–O–C structure, which then shifted up the valence band edge and reduce the band gap.

Figure 3c gives the photoelectricity results of the P25 and P25/graphene composite using a photocurrent test with a cutoff filter. The potential of the working electrode against a Pt counter electrode is set at 0.0 V. It is observed that there is a fast and uniform photocurrent responding to each switch-on and switch-off event in both electrodes. The photocurrents of the pure P25 and P25/graphene composites are 0.01 and 0.15 μA, respectively. Obviously, the photocurrent of the P25/graphene composites in visible light has been extremely improved as large as 15 times. Figure 3d is the decompositions of MB in the visible light. For the P25/graphene composite, about 70% of MB solutions were degraded after 5 h irradiation; in contrast, only 10% of MB solutions were degraded for the pure P25. The reasons for these improvements are attributed to the following mechanisms:

1. The formation of Ti–O–C bond or C-doped TiO_2 results in the absorbance edge of TiO_2 shifting to the higher wavelength region, and thereby increases the visible light photocatalytic activity.
2. Graphene possesses a remarkable electrical transport property. In the P25/graphene composite, the portion of graphene plays a role for conducting electrons, which makes the photocarrier transferring to the surface of graphene, and improves the separation of the electron–hole pairs and also the photocatalytic efficiency.
3. Graphene is of great specific surface area and strong capacity of absorption. Table 1 lists the specific surface area of graphene, P25, and P25/graphene composite,

Table 1 The specific surface area of the graphene, P25 TiO_2, and P25 TiO_2/graphene composite, respectively

	Graphene	P25	P25/graphene
Specific surface area ($m^2\ g^{-1}$)	757.380	55.725	78.678

respectively. The results show that the specific surface area of the reduced GO reaches up to 757.380 g m^{-2}, which is coincident to the current literature [7]. Therefore, graphene attributes to increase specific surface area of the composite. During degradation, at first, MB molecules were absorbed on the graphene surface, and reacted with the photocarrier transferred from TiO_2. Thus, graphene is taken as a carrier of photocatalysis, which can also accelerate the photocatalytic reaction rate greatly.

In addition, it has been known that the electronic structure of graphene is strongly associated with its number of layers. In general, a multi-layer graphene becomes a semimetal with a complex band structure in which the conduction and valence bands overlapping. This means that graphene can also absorb the visible light, and its excitation electrons are subsequently injected into the conduction band of TiO_2, and then transferred to the surface where they react with oxygen to yield superoxide radicals [23], and oxidize the MB directly.

Conclusions

A TiO_2 (P25)/graphene composite with a remarkable visible light photocatalytic activity was prepared using a process of heat treatment of GO. During photocatalyzing, graphene exhibits an ideal carrier for photocatalyst and plays a key role in the aspects of adsorption of MB molecules, separation of electron–hole pairs, and improvement of the visible light absorption due to C doping in the TiO_2 surface.

Acknowledgement This study was supported by the National Basic Research Program of China (973 Program) (No. 2009CB939704 and 2009CB939705).

References

1. Chen X, Mao SS (2007) Chem Rev 107:2891
2. Liu G, Wang L, Yang HG, Cheng HM, Lu GQ (2010) J Mater Chem 20:831
3. Wei HY, Wu YS, Lun N, Zhao F (2004) J Mater Sci 39:1305. doi:10.1023/B:JMSC.0000013889.63705.f3
4. Wu W, Cai YW, Chen JF, Shen SL, Martin A, Wen LX (2006) J Mater Sci 41:5845. doi:10.1007/s10853-006-0288-0
5. Balandin AA, Ghosh S, Bao W, Calizo I, Teweldebrhan D, Miao F, Laul CN (2008) Nano Lett 8:902
6. Bolotin KI, Sikes KJ, Jiang Z, Klima M, Fudenberg G, Hone J, Kim P, Stormer HL (2008) Solid State Commun 146:351
7. Peter S, Rainer W, Ralf T, Rolf M (2009) Macromol Rapid Commun 30:316
8. Klintenberg M, Lebegue S, Ortiz C, Sanyal B, Fransson J, Eriksson O (2009) J Phys Condens Matter 21:335502
9. Kothari AK, Konca E, Sheldon BW, Jian K, Li H, Xia Z, Ni W, Hurt R (2009) J Mater Sci 44:6020. doi:10.1007/s10853-009-3811-2
10. Jiang BZ, Zhamu A (2008) J Mater Sci 43:5092. doi:10.1007/s10853-008-2755-2
11. Zhang H, Lv X, Li Y, Wang Y, Li J (2010) ACS Nano 4:380
12. Zhang XY, Li HP, Cui XL, Lin Y (2010) J Mater Chem 20:2801
13. Hummers WS, Offeman RE (1958) J Am Chem Soc 80:1339
14. Kovtyukhova NI, Ollivier PJ, Martin BR, Mallouk TE, Chizhik SA, Buzaneva EV, Gorchinskiy AD (1999) Chem Mater 11:771
15. McAllister MJ, Li J, Adamson DH, Schniepp HC, Abdala AA, Liu J, Alonso MH, Milius DL, Car R, Prud'homme RK, Aksay IA (2007) Chem Mater 19:4396
16. Schniepp HC, Li J, McAllister MJ, Sai H, Alonso MH, Adamson DH, Prud'homme RK, Car R, Saville DA, Aksay IA (2006) J Phys Chem B 110:8535
17. Zhang T, Zhang D, Shen M (2009) Mater Lett 63:2051
18. Si Y, Samulski ET (2008) Nano Lett 8:1679
19. Bao Q, Bao S, Li CM, Qi X, Pan C, Zang J, Lu Z, Li Y, Tang DY, Zang S, Lian K (2008) J Phys Chem C 112:3612
20. Wang Y, Shao Y, Matson DW, Li J, Lin Y (2010) ACS Nano 4:1790
21. Zhang J, Pan C, Fang P, Wei J, Xiong R (2010) ACS Appl Mater Interfaces 2:1173
22. Wan L, Li JF, Feng JY, Sun W, Mao ZQ (2007) Mater Sci Eng B 139:216
23. Zhang LW, Fu HB, Zhu YF (2008) Adv Funct Mater 18:2180